Available online at www.sciencedirect.com

ScienceDirect

Nuclear Physics B 881 (2014) 327–342

NUCLEAR PHYSICS B

www.elsevier.com/locate/nuclphysb

Thermodynamic behavior of the generalized scalar Yukawa model in a magnetic background

L.M. Abreu [a,*], A.P.C. Malbouisson [b], J.M.C. Malbouisson [a], E.S. Nery [a], R. Rodrigues da Silva [c]

[a] *Instituto de Física, Universidade Federal da Bahia, 40210-340 Salvador, BA, Brazil*
[b] *Centro Brasileiro de Pesquisas Físicas, MCTI, 22290-180 Rio de Janeiro, RJ, Brazil*
[c] *Unidade Acadêmica de Física, Universidade Federal de Campina Grande, Campina Grande, PB, Brazil*

Received 27 January 2014; accepted 12 February 2014

Available online 18 February 2014

Abstract

We study the thermodynamic behavior of the generalized scalar Yukawa model, composed of a complex scalar field interacting with scalar and vector fields. Thermal effects are treated in the framework of generalized zeta-functions. For the case of vanishing effective chemical potential, we find a vanishing contribution from the vector field. We focus on the analysis of the phase structure of this model at effective chemical equilibrium, under change of values of the relevant parameters of the model, looking specially to the influence of the magnetic background on the phase structure.

Keywords: Finite-temperature field theory; Scalar Yukawa model

1. Introduction

Over the last decades a great interest has been driven to studies about phase diagrams of interacting relativistic systems under extreme conditions. The most efficient theoretical tool used to perform these studies is based on the formalism of relativistic quantum field theories at finite

* Corresponding author.
E-mail addresses: luciano.abreu@ufba.br (L.M. Abreu), adolfo@cbpf.br (A.P.C. Malbouisson), jmalboui@ufba.br (J.M.C. Malbouisson), elenilsonnery@hotmail.com (E.S. Nery), romulo@df.ufcg.edu.br (R. Rodrigues da Silva).

http://dx.doi.org/10.1016/j.nuclphysb.2014.02.013

temperature and density. These have been important in the understanding of many physical situations, such as cosmological problems, nuclear matter properties, relativistic degenerate gas processes, deconfinement–confinement phase transition involving strongly interacting matter, quark–gluon plasma formation in heavy-ion collisions (see Refs. [1,2] for reviews).

In particular, scalar quantum field theories have been frequently employed as a testing ground in describing relativistic systems. The absence of spin degrees of freedom means that these theories are relatively simple from both mathematical and conceptual points of view. In a theoretical perspective, they are commonly used as "laboratories" of more realistic theories to elaborate and to test the various techniques and non-perturbative approaches in Quantum Field Theory.

An example is the scalar Yukawa model, which describes the interaction between charged and neutral scalar bosons. It is the simplest model of the interaction between fields, and is often used as the prototype of more realistic theories in many situations. In the literature several scenarios are present, in which this model is applied; some of these are: nuclear physics (as a simplified version of the Yukawa model without spin degrees of freedom) and bound states of relativistic n-body systems [3–14]; hadron spectrum [15,16]; the effective interaction of scalar quarks in supersymmetric models [17,18]; phase transitions of relativistic systems under the change of magnitude of the interaction [19]; thermodynamic behavior of mesonic systems [20,21].

Interesting aspects, such as the investigation of phase diagrams, can be performed using the scalar Yukawa-like model, under the change of certain parameters, like finite temperature, finite chemical potential, and a magnetic background. In the spirit of a theoretical "laboratory" mentioned above, this study can be performed to give us, analytically, insights on the behavior of relativistic systems.

Thus, in this framework we study the thermodynamic behavior of a generalized version of the scalar Yukawa model, constituted of one complex scalar field interacting with real scalar and vector fields. In this context, we are interested on the properties of the matter composed of particles represented by the complex field, interacting via the exchange of scalar and vector particles. From a mathematical point of view, we make use of the zeta-function regularization approach. We investigate the phase transitions induced by the variation of temperature, chemical potential and external magnetic field, considering the interaction with real scalar and vector fields in the mean-field approximation. Here, this approximation means that we will neglect the fluctuations of the real scalar and vector fields. This represents charged scalar particles (associated to a complex scalar field) immersed in a background-medium of real scalar and vector particles. This constitutes the simplest way to parameterize the field equations of the complex scalar field taking into account the interaction with the other bosons.

On physical grounds, one of the possible physical applications of the situation mentioned above is on the description of a thermal gas of different types of particles interacting among them. An example is a system composed of heavy mesons (as for instance charmed mesons) interacting with a hadronic medium composed of light mesons. The motivation is the use of effective models to study the properties of hadronic matter with Yukawa-like interactions, in which D-mesons dominantly interact via the exchange of σ (simulating the two-pion exchange) and ω mesons [22]. In this sense, in our approach the complex scalar field would represent the D-meson; the real scalar and vector fields could be interpreted as the scalar meson σ (corresponding to a resonance in $\pi\pi$ scattering) and to the ω meson, respectively. Thus, the use of mean-field approximation would provide a first-order estimate of the thermodynamic properties D-meson matter.

The organization of this paper is as follows. In Section 2, we present the Lagrangian density and the other quantities describing the generalized version of the scalar Yukawa model, and

calculate the relevant quantities via the zeta-function regularization approach. The analysis of the thermodynamics of this bosonic gas is discussed in Section 3; in Section 4 this approach is extended to explore the dependence of the phase structure with a uniform magnetic background. Finally, Section 5 presents some concluding remarks.

2. The formalism

We consider a bosonic system interacting with pseudo-Goldstone bosons. We take as elementary objects of our model, a complex scalar field, a real pseudoscalar field and a massive vector field, respectively, ϕ, σ and ω^μ. We start by introducing the effective Lagrangian density,

$$\mathcal{L} = \big(\partial_\mu\phi^\dagger\big)\big(\partial^\mu\phi\big) - m_\phi^2\phi^\dagger\phi + \frac{1}{2}(\partial_\mu\sigma)\big(\partial^\mu\sigma\big) - \frac{1}{2}m_\sigma^2\sigma^2 + g_\sigma\phi^\dagger\phi\sigma - \frac{1}{4}W_{\mu\nu}W^{\mu\nu} + \frac{1}{2}m_\omega^2\omega_\mu\omega^\mu + ig_\omega\omega^\mu\big[\phi^\dagger\partial_\mu\phi - \big(\partial_\mu\phi^\dagger\big)\phi\big], \tag{1}$$

where $W^{\mu\nu} = \partial^\mu\omega^\nu - \partial^\nu\omega^\mu$, m_ϕ, m_ω and m_σ are respectively, the masses of the ϕ, σ and ω fields, and g_σ and g_ω are the coupling constants for the Yukawa-like interactions $\phi^\dagger\phi\sigma$ and $\phi^\dagger\phi\omega$.

In the Lorentz gauge, i.e. $\partial_\mu\omega^\mu = 0$, the equations of motion obtained from Eq. (1) are

$$\partial_\mu\partial^\mu\sigma + m_\sigma^2\sigma = g_\sigma\phi^\dagger\phi, \tag{2}$$

$$\partial_\mu\partial^\mu\omega^\nu + m_\sigma^2\omega^\nu = -ig_\omega\big[\phi^\dagger\partial^\nu\phi - \big(\partial^\nu\phi^\dagger\big)\phi\big], \tag{3}$$

and

$$\partial'_\mu\partial'^\mu\phi + \big(m_\phi^2 - g_\sigma\sigma + g_\omega^2\omega^\mu\omega_\mu\big)\phi = 0, \tag{4}$$

where $\partial'_\mu = \partial_\mu + ig_\omega\omega_\mu$; this "covariant" derivative describing the coupling between ϕ and ω^μ fields mimics a minimal gauge coupling. Unless explicitly stated, natural units, $\hbar = c = k_B = 1$ will be used all along the paper.

We are interested on the thermodynamic properties of the ϕ-field interacting with other fields. As a physical motivation, this can be thought of as representing scalar charged particles interacting with a background composed of neutral scalar and vector bosons. In this context, lowest order estimates for quantities describing the thermodynamics of the system can be obtained by using the mean-field approximation [23]. It means that we will neglect the fluctuations of the real scalar and vector fields, replacing the σ- and ω-fields by classical fields,

$$\bar{\sigma} = \langle\sigma\rangle, \qquad \bar{\omega} = \langle\omega^0\rangle, \tag{5}$$

with $\omega^\mu = 0$ for $\mu \neq 0$. This approximation allows us to rewrite the Lagrangian density in Eq. (1) as

$$\mathcal{L} = \phi^\dagger\big[-\partial_\mu\partial^\mu - \big(m_\phi^2 - g_\sigma\sigma\big)\big]\phi + \frac{1}{2}m_\omega^2\bar{\omega}^2 - \frac{1}{2}m_\sigma^2\bar{\sigma}^2 - g_\omega\bar{\omega}j^0, \tag{6}$$

where $j^0 = i[\phi^\dagger\partial^0\phi - (\partial^0\phi^\dagger)\phi]$. Besides, it can be seen from Eqs. (2)–(4) that, in mean-field approximation, $\bar{\sigma} \propto \rho_s$ and $\bar{\omega} \propto \rho$, with ρ_s and ρ being the scalar and number densities, respectively.

To study the thermodynamic behavior, we assume that the bosonic system is in thermodynamic equilibrium at a finite temperature T and at finite chemical potential (density) μ. Then, in

the framework of the imaginary time (Matsubara) formalism, the grand partition function takes the form [1,2],

$$\mathcal{Z} \propto \int \mathcal{D}\phi^{\dagger}\,\mathcal{D}\phi \exp\left\{-\int_0^{\beta} d\tau \int d^3x[\mathcal{L}_E + \mu j_0]\right\}, \tag{7}$$

where $\beta = 1/T$, and $\mathcal{L}_E$ is the Lagrangian density given by Eq. (6) in Euclidean space. Then, after integration over the fields ϕ and $\phi^{\dagger}$ the thermodynamic potential becomes,

$$\begin{aligned} U(T,\mu) &= V\left[\frac{1}{2}m_{\sigma}^2\bar{\sigma}^2 - \frac{1}{2}m_{\omega}^2\bar{\omega}^2\right] \\ &\quad + \frac{V}{\beta}\sum_{n=-\infty}^{\infty}\int \frac{d^3p}{(2\pi)^3}\ln\left\{\left[\frac{2\pi n}{\beta} - i\mu_{eff}\right]^2 + p^2 + m_{eff}^2\right\}, \end{aligned} \tag{8}$$

where V is the volume and m_{eff}^2 and μ_{eff} are respectively, the effective squared mass and the effective chemical potential of the scalar field ϕ; they read,

$$\begin{aligned} m_{eff}^2 &= m_{\phi}^2 - g_{\sigma}\bar{\sigma}, \\ \mu_{eff} &= \mu - g_{\omega}\bar{\omega}. \end{aligned} \tag{9}$$

In order to obtain the thermodynamic potential in a more tractable form, we use zeta-function regularization techniques [24–27]. In this scenario, Eq. (8) can be rewritten as

$$U(T,\mu) = V\left(\frac{1}{2}m_{\sigma}^2\bar{\sigma}^2 - \frac{1}{2}m_{\omega}^2\bar{\omega}^2\right) - \frac{V}{\beta}Y'(0), \tag{10}$$

where the zeta function $Y(s)$ is given by

$$\begin{aligned} Y(s) &= \sum_{n=-\infty}^{+\infty}\int \frac{d^3p}{(2\pi)^3}\left[\left(\frac{2\pi n}{\beta} - i\mu_{eff}\right)^2 + p^2 + m_{eff}^2\right]^{-s} \\ &= \frac{\Gamma(s-\frac{3}{2})}{(4\pi)^{3/2}\Gamma(s)}\sum_{n=-\infty}^{+\infty}\left[\left(\frac{2\pi n}{\beta} - i\mu_{eff}\right)^2 + m_{eff}^2\right]^{-s+\frac{3}{2}}, \end{aligned} \tag{11}$$

and $Y'(s)$ denotes the derivative of $Y(s)$ with respect to the argument s.

Then, by using the identity [24]

$$\begin{aligned} \sum_{n=-\infty}^{+\infty}\left[a(n-c)^2 + q^2\right]^{-\eta} &= \sqrt{\frac{\pi}{a}}\frac{\Gamma(\eta-\frac{1}{2})}{\Gamma(\eta)}q^{1-2\eta} + \frac{4\pi^{\eta}}{\sqrt{a}\Gamma(\eta)} \\ &\quad \times \sum_{n=1}^{\infty}\cos(2\pi nc)\left(\frac{n}{\sqrt{a}q}\right)^{\eta-\frac{1}{2}}K_{\eta-\frac{1}{2}}\left(\frac{2\pi nq}{\sqrt{a}}\right), \end{aligned} \tag{12}$$

and after some manipulations, the thermodynamic potential in Eq. (10) becomes

$$\begin{aligned} U(T,\mu) &= V\left(\frac{1}{2}m_{\sigma}\bar{\sigma}^2 - \frac{1}{2}m_{\omega}\bar{\omega}^2\right) + U_{vac} \\ &\quad - \frac{V}{\pi^2}\sum_{n=1}^{\infty}\cosh(\beta n\mu_{eff})\left(\frac{m_{eff}}{n\beta}\right)^2 K_2(n\beta m_{eff}), \end{aligned} \tag{13}$$

where K_ν is the modified Bessel function of the second kind, and U_{vac} is the (T, μ)-independent vacuum contribution which comes from the first term in the right hand side of Eq. (12). The term U_{vac} can be written, using a cutoff (Λ) regularization, as [28]

$$U_{vac} = \frac{1}{64\pi^2}\left\{2m_{eff}^2\Lambda^2 - \Lambda^4 + 2m_{eff}^4 \ln\left(m_{eff}^2\right) + 2\left(\Lambda^4 - m_{eff}^4\right)\ln\left(m_{eff}^2 + \Lambda^2\right)\right\}. \tag{14}$$

We will omit this term henceforth, which can be interpreted as a renormalization by minimal subtraction.

To proceed with the study of the thermodynamics of the model, we perform an analysis of the gap equations,

$$\frac{\partial U}{\partial \bar{\sigma}} = 0, \tag{15}$$

$$\frac{\partial U}{\partial \bar{\omega}} = 0. \tag{16}$$

The solutions of these equations give the values for $\bar{\sigma}$ and $\bar{\omega}$ that correspond to extremum points the thermodynamic potential U. Replacing Eq. (13) into the gap equations (15) and (16), yields,

$$\bar{\sigma} = \frac{g_\sigma}{m_\sigma^2}\rho_s, \tag{17}$$

$$\bar{\omega} = -\frac{g_\omega}{m_\omega^2}\rho, \tag{18}$$

where the scalar and number densities are written as

$$\rho_s = \frac{m_{eff}}{2\pi^2\beta}\sum_{n=1}^{\infty}\cosh\left(\beta n\mu_{eff}\right)\frac{1}{n}K_1(n\beta m_{eff}), \tag{19}$$

$$\rho = -\frac{m_{eff}^2}{\pi^2\beta}\sum_{n=1}^{\infty}\sinh\left(\beta n\mu_{eff}\right)\frac{1}{n}K_2(n\beta m_{eff}). \tag{20}$$

As remarked before, we have omitted the contribution coming from the vacuum term. It is worth to mention that if the numbers of ϕ-particles and antiparticles are equal, which means a vanishing effective chemical potential $\mu_{eff} = 0$, we see from Eqs. (18) and (20) that $\rho = 0$ and therefore $\bar{\omega} = 0$.

All other relevant thermodynamic quantities can be derived from the thermodynamic potential given by Eq. (13). For instance, the pressure reads

$$p(T,\mu) \equiv -\frac{\partial U}{\partial V} = \frac{1}{2}m_\omega\bar{\omega}^2 - \frac{1}{2}m_\sigma\bar{\sigma}^2 + \frac{1}{\pi^2}\sum_{n=1}^{\infty}\cosh\left(\beta n\mu_{eff}\right)\left(\frac{m_{eff}}{n\beta}\right)^2 K_2(n\beta m_{eff}). \tag{21}$$

Therefore, the values of $\bar{\sigma}$ and $\bar{\omega}$ corresponding to extremum points of the pressure must also satisfy Eqs. (17) and (18).

In addition, the entropy and energy densities at chemical equilibrium are given by,

$$s(T) \equiv \left.\frac{\partial p}{\partial T}\right|_{\mu_{eff}=0} = \frac{1}{\pi^2}\sum_{n=1}^{\infty}\frac{m_{eff}^3}{n}K_3(n\beta m_{eff}), \tag{22}$$

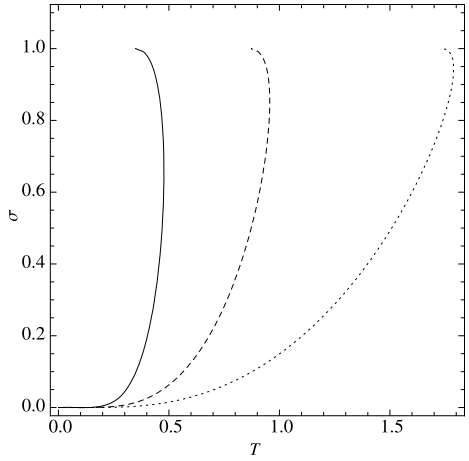

Fig. 1. Plot of $\bar{\sigma}$ in Eq. (17) (after scaling by Eq. (24)) as a function of temperature, at chemical equilibrium, for $m_\sigma = 0.1, 0.25$ and 0.5 (respectively full, dashed and dotted lines). We fix $g_\sigma = 1.0$.

and

$$\varepsilon(T) \equiv (-p + Ts)_{\mu_{eff}=0} = \frac{1}{2} m_\sigma \bar{\sigma}^2 + \frac{1}{\pi^2} \sum_{n=1}^{\infty} \left[3 \left(\frac{m_{eff}}{n\beta} \right)^2 K_2(n\beta m_{eff}) + \frac{m_{eff}^3}{n\beta} K_1(n\beta m_{eff}) \right], \tag{23}$$

respectively.

3. Thermodynamic behavior

We now analyze the thermodynamic behavior of the model. We consider the case of null chemical potential, $\mu_{eff} = 0$, where the number of ϕ-bosons and anti-bosons are equal in the mesonic medium. Let us write all physical quantities in units of the mass of the scalar field ϕ, m_ϕ. We have,

$$\frac{U}{m_\phi^4} \to U, \qquad \frac{T}{m_\phi} \to T, \qquad \frac{\nu}{m_\phi} \to \nu, \qquad \frac{\sigma}{m_\phi} \to \sigma,$$
$$\frac{m_{eff}}{m_\phi} \to m_{eff}, \qquad \frac{g_\sigma}{m_\phi} \to g_\sigma, \qquad \frac{m_\sigma}{m_\phi} \to m_\sigma. \tag{24}$$

Since we are interested in the general thermodynamic behavior of the model, we perform an analysis using different values of the relevant parameters. In what follows, including the figures, all those parameters are understood to be redefined by the scaling in Eq. (24).

In Fig. 1, it is plotted the field $\bar{\sigma}$ in Eq. (17) as a function of temperature, for three values of the mass of the σ-field, m_σ: 0.1, 0.25 and 0.5, at chemical equilibrium, that is $\mu_{eff} = 0$. The value of g_σ is 1.0. We note that $\bar{\sigma}$ does not exist for temperatures above the values $T \approx 0.47$, 0.96 and 1.79, for $m_\sigma = 0.1$, 0.25 and 0.5, respectively. Besides, $\bar{\sigma}$ has a maximum value at $T \equiv T_D \approx 0.34$, 0.87 and 1.76, for the three cases mentioned above. At the critical value T_D, we have a vanishing effective mass. Notice that this critical temperature can be obtained analytically

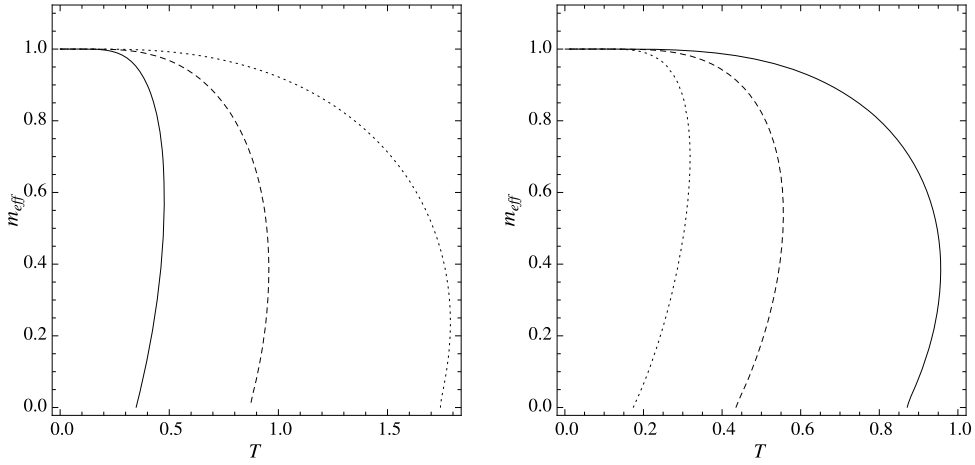

Fig. 2. Plot of effective mass in Eq. (17) as a function of temperature, at chemical equilibrium. Left panel: we fix $g_\sigma = 1.0$, with full, dashed and dotted lines representing respectively $m_\sigma = 0.1$, 0.25 and 0.5. Right panel: we fix $m_\sigma = 0.25$, with full, dashed and dotted lines representing respectively $g_\sigma = 1.0$, 2.0 and 5.0.

by taking $m_{eff} \approx 0$ in Eqs. (17) and (19) and using the asymptotic formula for small values of the argument of the Bessel function,

$$K_\nu(z) \approx \frac{1}{2}\Gamma(\nu)\left(\frac{z}{2}\right)^{-\nu} \quad \big(z \sim 0; \mathrm{Re}(\nu) > 0\big). \tag{25}$$

We get,

$$\bar{\sigma} = \frac{g_\sigma T^2}{2m_\phi^2 m_\sigma^2 \pi^2}\zeta(2), \tag{26}$$

where $\zeta(s)$ is the Riemann *zeta*-function, with the particular value $\zeta(2) = \pi^2/6$. Then from Eqs. (26) and (9), remembering the scaling (24), we have

$$T_D = \sqrt{12}\frac{m_\sigma}{g_\sigma}. \tag{27}$$

For the values of the parameters mentioned above, we obtain values of T_D in agreement with those in Fig. 1. We also see from Fig. 1 that as m_σ increases the critical temperature increases.

Let us now turn our attention to the behavior of the effective mass of the ϕ-field in a medium. We plot in the left panel of Fig. 2 the values for m_{eff} that are solutions of the gap equation (17) as a function of temperature, for different values of the mass of the σ-field. We can see that the effective mass reduces as the temperature increases, and a transition from an interacting gas to a strongly interacting matter appears at the temperature T_D (similar to a liquid–gas transition).

In the right panel of Fig. 2, it is plotted the effective mass as a function of temperature by taking different values of the coupling constant g_σ. It can be seen that the critical temperature decreases as g_σ increases, in agreement with Eq. (27). For instance, with $g_\sigma = 2.0$ and 5.0 in Eq. (27) we get $T_D \approx 0.43$ and 0.17, respectively. This fact makes explicit the role of the σ field in binding the ϕ-bosons; the increasing of the magnitude of the interaction between the σ and ϕ fields makes the system to undergo a phase transition at a smaller temperature.

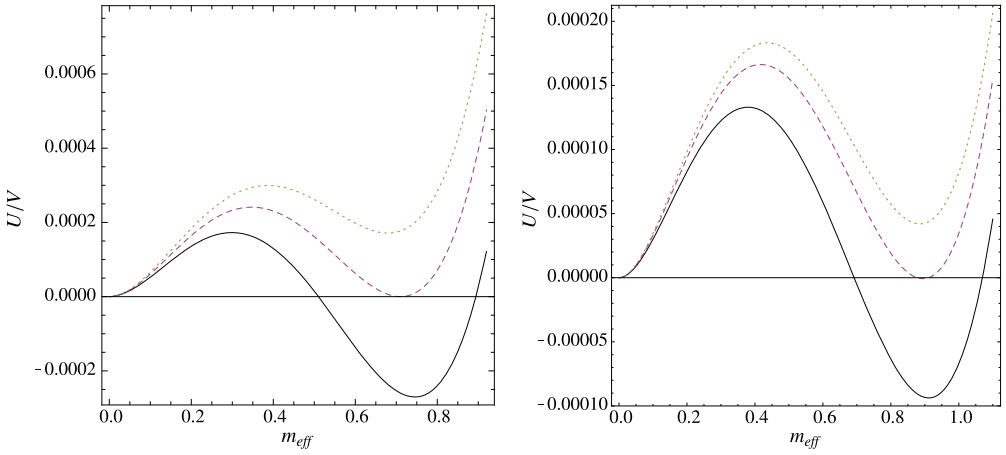

Fig. 3. Plot of thermodynamic potential density of Eq. (13) as a function of effective mass, at chemical equilibrium, for $m_\sigma = 0.25$. Left panel: we use $g_\sigma = 2.0$, with full, dashed and dotted lines representing the cases for $T = 0.53$, 0.539 and 0.545, respectively. Right panel: we use $g_\sigma = 5.0$, with full, dashed and dotted lines representing the cases for $T = 0.285$, 0.292 and 0.295, respectively.

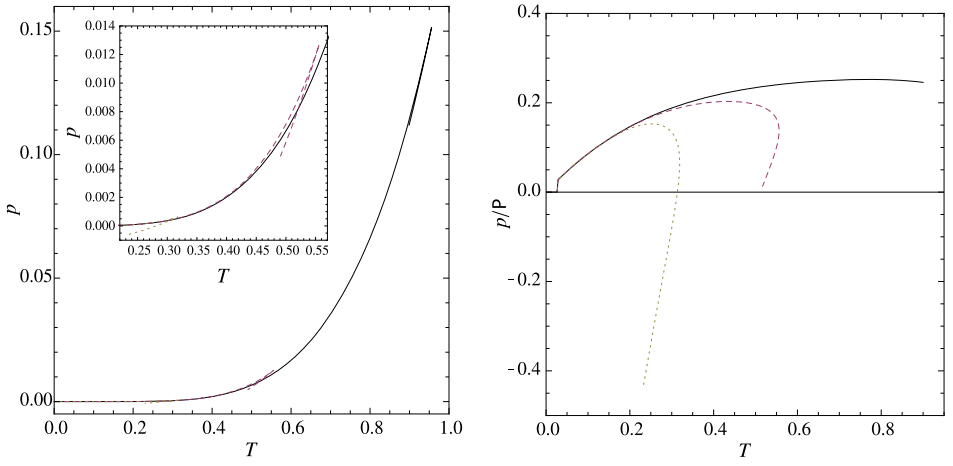

Fig. 4. Left panel: Plot of pressure in Eq. (21) as a function of temperature, at chemical equilibrium. In detail, the plot in the range of temperature 0.22 to 0.56. Right panel: Ratio of pressure/energy density as a function of temperature at chemical equilibrium. Full, dashed and dotted lines represent $g_\sigma = 1.0$, 2.0 and 5.0 respectively. We fix $m_\sigma = 0.25$.

To proceed with the characterization of the thermodynamics of this system, in Fig. 3 the thermodynamic potential density $U(T, \mu)/V$ from Eq. (13) is plotted as a function of effective mass for $g_\sigma = 2.0$ and 5.0, respectively, and for $m_\sigma = 0.25$. As suggested in the previous figures, we observe a first-order phase transition occurring at $T_0 \approx 0.54$, when the mass acquires the value $m_{eff} \approx 0.71$ in the case $g_\sigma = 2.0$. For $g_\sigma = 5.0$, a discontinuous phase transition occurs at $T_0 \approx 0.29$, when the mass acquires the value $m_{eff} \approx 0.91$. Thus, we find that the first-order transition occurs at a lower temperature as the value of the coupling constant g_σ increases.

In Fig. 4 it is plotted the pressure from Eq. (21) as a function of temperature for different values of g_σ: 1.0, 2.0 and 5.0. We can see that for larger values of the coupling constant, the

pressure can assume negative values. This result suggests that a stronger interaction between the ϕ-bosons induces a phase transition from a gas-like state into a condensed-like matter state with negative pressure. This can be seen still more clearly from the plot of the ratio of pressure to energy density, given in the right panel of Fig. 4 for different values of the coupling constant. We can also see that for larger values of g_σ the range of allowed values of P/ρ is such that, both its maximum (positive) and the attained negative values are smaller.

4. System under the influence of a magnetic background

Another interesting aspect of the properties of the system considered here are the changes induced by the presence of a magnetic background. To analyze the role of an external magnetic field, we must consider the modified Lagrangian density,

$$\begin{aligned}\mathcal{L} &= (D_\mu\phi)^\dagger\left(D^\mu\phi\right) - m_\phi^2\phi^\dagger\phi + \frac{1}{2}(\partial_\mu\sigma)\left(\partial^\mu\sigma\right) - \frac{1}{2}m_\sigma^2\sigma^2 \\ &\quad - \frac{1}{4}W_{\mu\nu}W^{\mu\nu} + \frac{1}{2}m_\omega^2\omega_\mu\omega^\mu + g_\sigma\phi^\dagger\phi\sigma + ig_\omega\omega^\mu\left[\phi^\dagger\partial_\mu\phi - \left(\partial_\mu\phi^\dagger\right)\phi\right],\end{aligned} \tag{28}$$

where

$$D_\mu = \partial_\mu + ieA_\mu^{ext}.$$

Then, the ϕ-field minimally coupled to the external magnetic field satisfies the following equation of motion in mean-field approximation,

$$\left(\partial_\mu + ieA_\mu^{ext}\right)\left(\partial^\mu + ieA_{ext}^\mu\right)\phi + \left(m_\phi^2 - g_\sigma\bar{\sigma}\right)\phi + 2ig_\omega\bar{\omega}\partial_0\phi = 0. \tag{29}$$

In the above equations, we choose the gauge $A_{ext}^\mu = (0, -x_2H, 0, 0)$, where H is the intensity of the uniform external magnetic field, directed along the z-axis. In this case, the part of the Hamiltonian quadratic in ϕ becomes, after an integration by parts, $-\int d^Dr\,\phi^*\,\mathcal{D}\phi$, where we have the differential operator

$$\mathcal{D} = \nabla^2 - 2ieHx_1\partial_{x_2} - (eH)^2x_1^2 - {m_0}^2; \tag{30}$$

the natural basis to expand the field operators is the set of the normalized eigenfunctions of the operator $\mathcal{D}$, the Landau basis. This means that the solutions of Eq. (29) can be written in the form,

$$\phi(x) = e^{i(p_0x_0 - p_1x_1 - p_3x_3)}u(x_2), \tag{31}$$

where $u(x_2)$ satisfies a harmonic oscillator equation,

$$\left[-\partial_{x_2}^2 + e^2H^2\left(x_2 - \frac{p_1}{eH}\right)^2\right]u(x_2) = 0. \tag{32}$$

The solutions of Eq. (32) are,

$$u_l(x_2) = \frac{1}{\sqrt{2^l l!}}\left(\frac{eH}{\pi}\right)^{1/4}H_l\left[\sqrt{eH}\left(x_2 - \frac{p_1}{eH}\right)\right], \tag{33}$$

where H_l are Hermite polynomials. The corresponding energy spectrum provides the dispersion relation,

$$p_0^2 = p_3^2 + m_{eff}^2 + 2eH(2l+1), \tag{34}$$

with $l = 0, 1, 2, \ldots$, denoting the Landau levels.

Thus, magnetic effects, with the introduction of the Landau basis, implies in a change in the momentum space integrations of the type,

$$\int \frac{d^4p}{(2\pi)^4} f(p) \to \frac{eH}{2\pi} \sum_{l=0}^{\infty} \int \frac{d^2p}{(2\pi)^2} f(p_0, p_3, l).$$

This change, together with the results from Eq. (29) up to Eq. (34), leads to replace the zeta function $Y(s)$ (given by Eq. (11) in the absence of external field), by the modified zeta-function,

$$\begin{aligned} Z(s) &= \frac{\Gamma(s-\frac{1}{2})}{(4\pi)^{1/2}\Gamma(s)} \sum_{l=0}^{+\infty} \sum_{n=-\infty}^{+\infty} \left[\left(\frac{2\pi n}{\beta} - i\mu_{eff} \right)^2 + m_{eff}^2 + 2eH(2l+1) \right]^{-s+\frac{1}{2}} \\ &= eH \left[\frac{\beta}{8\pi^2} \frac{\Gamma(s-1)}{\Gamma(s)} F_1(s-1) + \frac{\beta}{\pi^2} \frac{1}{\Gamma(s)} F_2(s-1) \right], \end{aligned} \tag{35}$$

where the functions $F_1(\nu)$ and $F_2(\nu)$ are respectively,

$$F_1(\nu) = (2eH)^{-\nu} \zeta\left(\nu, \frac{1}{2} + \frac{m_{eff}^2}{2eH}\right), \tag{36}$$

$$F_2(\nu) = \sum_{l=0}^{\infty} \sum_{n=1}^{\infty} \cosh(n\mu_{eff}\beta) \left(\frac{n\beta}{2M_l} \right)^{\nu} K_\nu(n\beta M_l); \tag{37}$$

in the above equations $\zeta(\eta, a) = \sum_{k=0}^{\infty} (k+a)^{-\eta}$ is the generalized zeta-function, and

$$M_l = \sqrt{m_{eff}^2 + 2eH(2l+1)}. \tag{38}$$

In a similar way as in Eq. (10), in order to obtain the thermodynamic potential we must perform the derivative of $Z(s)$ with respect to s, for $s \to 0$. This operation can be shortened by analyzing the pole structure of Eq. (35) for $s \to \epsilon$ (with $\epsilon \ll 1$) [28],

$$\begin{aligned} \frac{d}{d\eta} \left[\frac{\Gamma(\eta-1)}{\Gamma(\eta)} F_1(\eta) \right]_{\eta\to\epsilon} &\approx F_1(\epsilon-1) - (1+\epsilon) F_1'(\epsilon-1), \\ \frac{d}{d\eta} \left[\frac{1}{\Gamma(\eta)} F_2(\eta-1) \right]_{\eta\to\epsilon} &\approx F_2(\epsilon-1). \end{aligned} \tag{39}$$

Then, for $\epsilon \to 0$, we obtain the (T, μ, H)-dependent thermodynamic potential,

$$\begin{aligned} U(T,\mu,H) = V &\left(\frac{1}{2} m_\sigma \bar{\sigma}^2 - \frac{1}{2} m_\omega \bar{\omega}^2 \right) + U_{vac} \\ &+ V \frac{(eH)^2}{4\pi^2} F_3\left(\frac{m_{eff}^2}{2eH} \right) - V \frac{2eH}{\pi^2} F_2(-1), \end{aligned} \tag{40}$$

where U_{vac} is the vacuum contribution (which will be omitted, as in previous section), and

$$F_3(z) = \zeta'\left(-1, \frac{1}{2} + z\right) - \frac{1}{2} z^2 \ln z + \frac{5}{4} z^2. \tag{41}$$

Thus, the gap equations in the presence of a magnetic background can be obtained by using Eq. (40) in (15) and (16), yielding,

$$\bar{\sigma} = \frac{g_\sigma}{m_\sigma^2}\rho_s^H, \tag{42}$$

$$\bar{\omega} = -\frac{g_\omega}{m_\omega^2}\rho^H, \tag{43}$$

where the H-dependent scalar and number densities are written as

$$\rho_s^H = -\frac{eH}{2\pi^2}\left[\frac{1}{4}F_4\left(\frac{m_{eff}^2}{2eH}\right) - F_2(0)\right], \tag{44}$$

$$\rho^H = -\frac{eH}{\pi^2}\sum_{l=0}^{\infty}\sum_{n=1}^{\infty}\sinh(\beta n\mu_{eff})M_l K_{-1}(n\beta M_l). \tag{45}$$

In Eq. (44) above we have introduced the function

$$F_4(z) = \ln\Gamma\left(\frac{1}{2}+z\right) - \frac{1}{2}\ln(2\pi) + z\ln z - 3z. \tag{46}$$

As in the absence of magnetic background, we find that at chemical equilibrium, i.e. $\mu_{eff} = 0$, Eqs. (43) and (45) imply that $\rho^H = 0$ and therefore $\bar{\omega} = 0$.

5. Thermodynamic behavior: dependence on the magnetic background

We now focus the analysis on the effective potential and the solutions of the gap equations, at chemical equilibrium, under change of values of the relevant parameters of the model, looking specially at the influence of the magnetic background on the phase structure. In the figures, the notations are the same as those already employed previously; in addition we introduce the notation $\Omega = eH$ standing for the so-called cyclotron frequency. We see from Eq. (34) that Ω has dimension of $mass^2$ and thus, since we are taking all physical quantities scaled by the ϕ-mass, m_ϕ, the cyclotron frequency will be a dimensionless parameter,

$$\frac{\Omega}{m_\phi^2} \to \Omega, \tag{47}$$

as the other quantities in Eq. (24).

In Fig. 5, the effective mass from Eq. (42) is plotted as a function of temperature, for different values of the external magnetic field. We find that at lower values of the magnetic field, the effective mass presents a behavior similar to the one in absence of magnetic background, studied previously: m_{eff} behaves in an analogous way as in the case of a liquid–gas transition. However, for larger values of Ω, we see that as the temperature increases, m_{eff} attains more rapidly a certain value where it begins to decrease in a way nearly independent of the temperature.

In order to better understand the nature of the phase transition region in connection with the points raised above, Figs. 6 and 7 display the thermodynamic potential density from Eq. (40) at different values of the temperatures in the transition region, with the magnetic field kept fixed in three different cases. We summarize some aspects that should be noticed. The main conclusions coming out from these figures are:

(i) For fixed values of Ω, there is a transition from the broken to the unbroken phase as the temperature increases, as in previous case in absence of magnetic field.
(ii) With the magnetic field kept at small values ($\Omega = 0.1$ and $\Omega = 0.25$ in Fig. 6), the system exhibits a first order phase transition as the temperature increases.

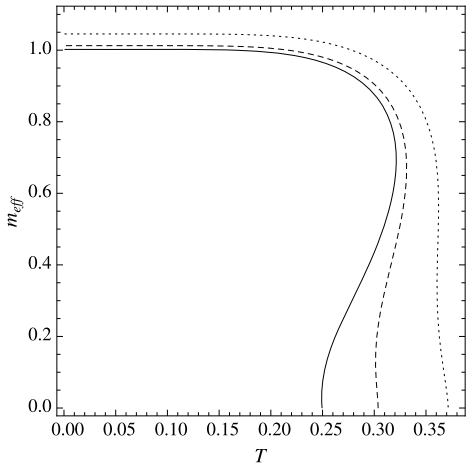

Fig. 5. Plot of effective mass in Eq. (42) as a function of temperature, at chemical equilibrium, for $\Omega = 0.1$, 0.25 and 0.5 (respectively full, dashed and dotted lines). We fix $g_\sigma = 5.0$.

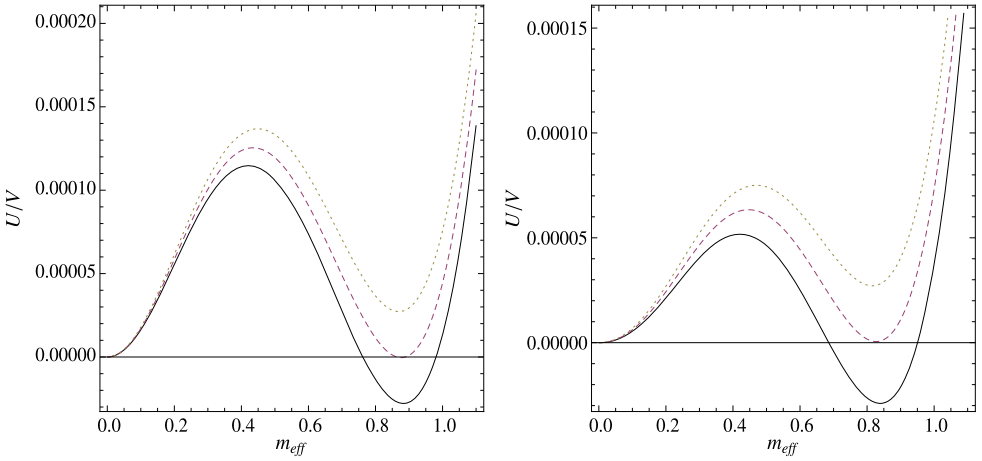

Fig. 6. Plot of thermodynamic potential density in Eq. (40) as a function of effective mass, at chemical equilibrium, for $m_\sigma = 0.25$ and $g_\sigma = 5.0$. Left panel: we fix $\Omega = 0.1$; full, dashed and dotted lines represent the cases for $T = 0.298$, 0.300 and 0.302, respectively. Right panel: we fix $\Omega = 0.25$; full, dashed and dotted lines correspond to $T = 0.318$, 0.320 and 0.322, respectively.

(iii) Also, as the magnetic field increases, the critical temperature at which the system undergoes the phase transition increases.

(iv) For larger values of the magnetic field (e.g. $\Omega = 0.5$ in Fig. 7), the system exhibits a "two-step phase transition" as the temperature increases. First, a discontinuous phase transition occurs with the equilibrium effective mass jumping to a smaller value; this happens at the temperature for which the two non-null local minima of the thermodynamic potential become degenerated. Further increasing the temperature, a continuous phase transition appears, with the absolute minimum, which gives the equilibrium value of m_{eff}, tending

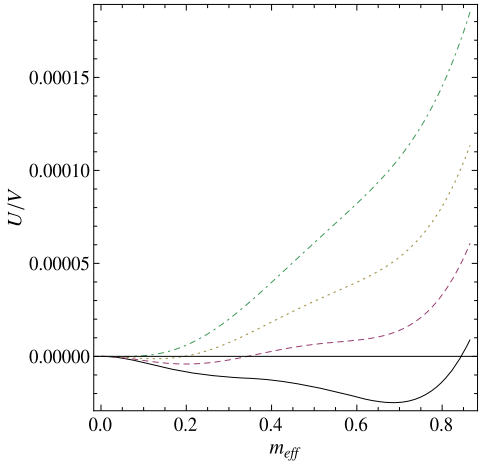

Fig. 7. Plot of thermodynamic potential density, Eq. (40), as a function of effective mass, at chemical equilibrium, for $m_\sigma = 0.25$ and $g_\sigma = 5.0$. We fix $\Omega = 0.5$; full, dashed, dotted and dot-dashed lines represent the cases for $T = 0.361$, 0.3615, 0.362 and 0.370, respectively.

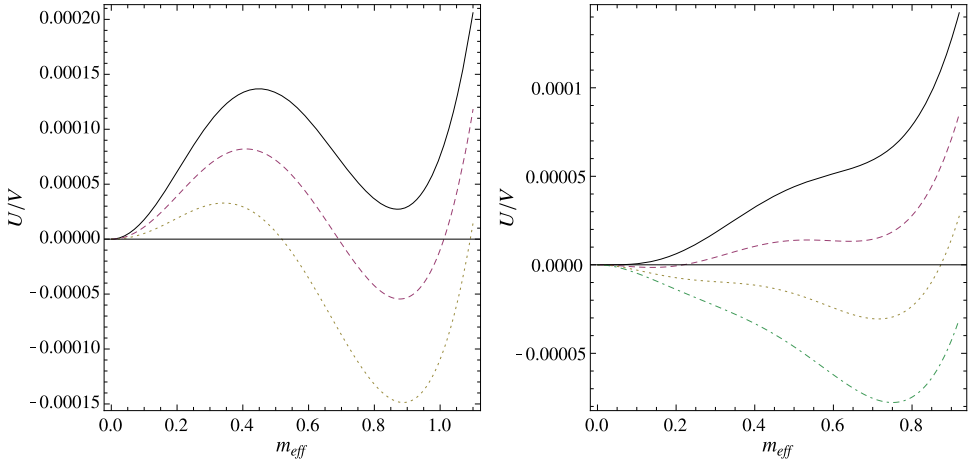

Fig. 8. Plot of thermodynamic-potential density, Eq. (40), as a function of effective mass, at chemical equilibrium, for $m_\sigma = 0.25$ and $g_\sigma = 5.0$. Left panel: we fix $T = 0.30$; full, dashed and dotted lines represent the cases for $\Omega = 0.08, 0.10$ and 0.12, respectively. Right panel: we fix $T = 0.36$; full, dashed, dotted and dot-dashed lines correspond to $\Omega = 0.470$, 0.490, 0.491 and 0.492, respectively.

to zero. It is worthy mentioning that a similar two-step transition is also found in a four-fermion interaction scenario [29].

In addition, the thermodynamic potential density, given by Eq. (40), is plotted in Fig. 8 as a function of m_{eff}, for different values of magnetic field, but with the temperature kept fixed in two different scenarios. The main conclusions coming out from these plots are:

(i) For fixed values of T, there is a transition from the unbroken to the broken phase driven by the enhancement of the magnetic field; that is, the increasing of the magnetic field tends to favor the ordered phase, in opposition to the raising of temperature which leads the system to the symmetry-restored phase. The favoring of the broken phase with the increasing of the applied magnetic field, known as magnetic catalysis, is also present in other situations, including fermionic systems [28–30,32,31,33]. The physical meaning of this effect is that the magnetic field drives the system to the ordered phase; the maintenance of long-range correlations is enhanced, favoring the ordering.
(ii) With the temperature kept low, the system exhibits a first order phase transition from the unbroken to the broken phase as the magnetic field increases.
(iii) As the temperature increases, the critical magnetic field at which the system undergoes the phase transition increases.
(iv) For higher temperatures, as the magnetic field increases the system exhibits again a two-step phase transition from the unbroken to the broken phase: the first being continuous phase transition, with the absolute minimum appearing for a non-null value of m_{eff}, and after a discontinuous transition, when the emergent second local minimum at a higher value of m_{eff} overcomes the first one, becoming the absolute minimum.

6. Concluding remarks

We have performed a study on the thermodynamic behavior of a generalized scalar Yukawa model, in which we consider a complex scalar field, ϕ, interacting with scalar and vector fields, σ and ω, respectively, in the mean field approximation. A possible application of this model is in the thermodynamic analysis of a gas composed of heavy-flavored and light mesons. From a technical point of view, we employ the effective potential formalism in the framework of the zeta-function regularization approach. We have shown that the ω-field does not contribute when the system has the same number of particles and antiparticles. On the other hand, the σ-field has a nontrivial solution coming from the gap equation, which grows as the temperature increases. For the case of vanishing effective chemical potential, we find that the contribution from the vector field is zero. Besides, the effective mass of the scalar field decreases as the temperature increases, signalizing a phase transition, which can be interpreted as the formation of exotic bound states at higher temperatures. Also, it has been shown that a first-order transition occurs at lower temperatures as the value of the coupling constant g_σ increases. This shows the significant role of the σ-field in binding the bosons, as the increasing of the magnitude of the interaction, induces the system to undergo a phase transition at a smaller temperature. In addition, in the case of stronger couplings, we can see from Fig. 4 that the pressure becomes negative for temperatures above the transition temperature T_c.

In what magnetic effects are concerned, one of the main conclusions we can extract from the model is the presence of what is known as "magnetic catalysis"; this means that, for fixed values of T, the broken phase is favored as the magnetic field is increased. Actually, this effect is also present in other situations including fermionic systems. Another interesting effect is that, for large enough values of the applied magnetic field, the system exhibits a two-step phase transition, as the temperature increases. For small values of the temperature, a discontinuous phase transition occurs. As the temperature is raised, a continuous phase transition appears, with the minimum of the thermodynamic potential growing from zero; for larger values of the external magnetic field, another local minimum develops at a higher value of m_{eff} and overcomes the first one, leading to a discontinuous jump in the equilibrium effective mass.

Finally, we discuss results of our model with respect to the application pointed out in the Introduction, i.e. a system of D-mesons in a medium of light mesons composed of σ- and ω-mesons. In this case we take $m_D = 1.87$ GeV [34], and choose $m_\sigma = 0.214 m_D \approx 0.4$ GeV and $g_\sigma = 5 m_D \approx 9.35$ GeV. Then, from Eq. (26) we obtain the critical temperature $T_c \approx 0.148 m_D \approx 277$ MeV. It is interesting to notice that calculations in lattice QCD suggest that the charmonium dissociation temperature has a value between $1.6 T_d$ and $2.35 T_d$ [35,36], where $T_d \approx 0.092 m_D \approx 172$ MeV is the deconfinement temperature [37]. Thus, in this scenario our results are in agreement with those in the literature. In addition, when we consider the influence of a magnetic background taking $\Omega = 0.035 m_D = 65$ MeV, the first-order phase transition occurs at a critical temperature of $T_c \approx 0.27 m_D \approx 505$ MeV.

Hence, we believe that the results summarized above give us insights on the behavior of relativistic systems, as a mesonic gas. Further studies must be done in order to improve this approach, as the inclusion of other interactions, and to perform the analysis beyond mean-field approximation.

Acknowledgements

This work has been partially supported by CNPq, CAPES/PROCAD-NF and FAPERJ, Brazilian agencies.

References

[1] M. Le Bellac, Thermal Field Theory, Cambridge University Press, Cambridge, 1996.
[2] J.I. Kapusta, C. Gale, Finite Temperature Field Theory: Principles and Applications, Cambridge University Press, Cambridge, 2006.
[3] J.W. Darewych, Can. J. Phys. 76 (1998) 523.
[4] G.V. Efimov, arXiv:hep-ph/9907483.
[5] B. Ding, J.W. Darewych, J. Phys. G, Nucl. Part. Phys. 26 (2000) 907.
[6] V. Shpytko, J. Darewych, Phys. Rev. D 64 (2001) 045012.
[7] A. Duviryak, J.W. Darewych, J. Phys. A, Math. Gen. 37 (2004) 8365.
[8] K. Barro-Bergflodt, R. Rosenfelder, M. Stingl, Few-Body Syst. 39 (2006) 193.
[9] M. Emami-Razavi, M. Kowalski, Phys. Rev. D 76 (2007) 045006.
[10] M. Emami-Razavi, Phys. Rev. D 77 (2008) 045025.
[11] M. Emami-Razavi, N. Bergeron, J.W. Darewych, M. Kowalski, Phys. Rev. D 80 (2009) 085006.
[12] M. Emami-Razavi, N. Bergeron, J.W. Darewych, J. Phys. G, Nucl. Part. Phys. 37 (2010) 025007.
[13] M. Emami-Razavi, N. Bergeron, J.W. Darewych, J. Phys. G, Nucl. Part. Phys. 38 (2011) 065004.
[14] A. Chigodaev, J.W. Darewych, Can. J. Phys. 91 (2013) 279;
A. Chigodaev, J.W. Darewych, Can. J. Phys. 91 (2013) 764.
[15] G.V. Efimov, G. Ganbold, Phys. Rev. D 65 (2002) 054012.
[16] G. Ganbold, Phys. Part. Nucl. 43 (2012) 79.
[17] J. Guasch, S. Peñaranda, R. Sanchez-Florit, J. High Energy Phys. 0904 (2009) 016.
[18] A. Abrahantes, J. Guasch, S. Peñaranda, R. Sanchez-Florit, Eur. Phys. J. C 73 (2013) 2368.
[19] V.E. Rochev, J. Phys. A, Math. Theor. 46 (2013) 185401.
[20] M.L.F. Freire, R. Rodrigues da Silva, AIP Conf. Proc. 1296 (2010) 346.
[21] L.M. Abreu, E.S. Nery, R. Rodrigues da Silva, arXiv:1211.5505, 2012.
[22] Gui-Jun Ding, Phys. Rev. D 79 (2009) 014001.
[23] J.D. Walecka, Ann. Phys. 83 (1974) 491.
[24] E. Elizalde, Ten Physical Applications of Spectral *zeta* Function, 2nd ed., Lecture Notes in Physics, vol. 855, Springer-Verlag, Berlin, 2012.
[25] T. Inagaki, T. Kouno, T. Muta, Int. J. Mod. Phys. A 10 (1995) 2241.
[26] L.M. Abreu, A.P.C. Malbouisson, J.M.C. Malbouisson, A.E. Santana, Nucl. Phys. B 819 (2009) 127.
[27] L.M. Abreu, A.P.C. Malbouisson, J.M.C. Malbouisson, Phys. Rev. D 83 (2011) 025001.

[28] L.M. Abreu, A.P.C. Malbouisson, J.M.C. Malbouisson, Phys. Rev. D 84 (2011) 065036.
[29] T. Inagaki, D. Kimura, T. Murata, Prog. Theor. Phys. 111 (2004) 371.
[30] D. Ebert, K.G. Klimenko, Nucl. Phys. A 728 (2003) 203.
[31] E.S. Fraga, A.J. Mizher, Phys. Rev. D 78 (2008) 025016.
[32] D.P. Menezes, M.B. Pinto, S.S. Avancini, A.P. Martínez, C. Providência, Phys. Rev. C 79 (2009) 035807.
[33] Sh. Fayazbakhsh, N. Sadooghi, Phys. Rev. D 83 (2011) 025026.
[34] J. Beringer, et al., Particle Data Group Collaboration, Phys. Rev. D 86 (2012) 010001.
[35] M. Asakawa, T. Hatsuda, Phys. Rev. Lett. 92 (2004) 012001.
[36] H.T. Ding, A. Francis, O. Kaczmarek, F. Karsch, H. Satz, W. Soeldner, Phys. Rev. D 86 (2012) 014509.
[37] V.G. Bornyakov, R. Horsley, Y. Nakamura, M.I. Polikarpov, P. Rakow, G. Schierholz, arXiv:1102.4461, 2011.